NASA TECHNICAL MEMORANDUM

NASA-TM-77380 19840011291

NASA TM-77380

USE OF ADAPTIVE WALLS IN 2D TESTS

J. P. Archambaud and J. P. Chevallier

Transation of "Utilisation de parois adaptables pour les essais en courant plan", Advisory Group for Aerospace Research and Development, In: Wall Interference in Wind Tunnels, Neuilly Sur Seine, France, AGARD-CP-335, September 1982, pp. 14-1 to 14-14.

REVISED VERSION

NATIONAL AERONAUTICS AND SPACE ADMINISTRATION
WASHINGTON, D.C. 20546 FEBRUARY 1984

STANDARD TITLE PAGE

1. Report No.	2. Government Accession No.	3. Recipient's Catalog No.
NASA TM 77380		

4. Title and Subtitle	5. Report Date
USE OF ADAPTIVE WALLS IN 2D TESTS	February 1984
	6. Performing Organization Code

7. Author(s)	8. Performing Organization Report No.
J.P. Archambaud and J.P. Chevallier	
	10. Work Unit No.

9. Performing Organization Name and Address	11. Contract or Grant No.
Leo Kanner Associates Redwood City, California 94063	NASw-3541
	13. Type of Report and Period Covered
	Translation
12. Sponsoring Agency Name and Address	14. Sponsoring Agency Code
National Aeronautics and Space Administration, Washington, D.C. 20546	

15. Supplementary Notes

Translation of "Utilisation de parois adaptables pour les essais en courant plan", Advisory Group for Aerospace Research and Development, In: Wall Interference in Wind Tunnels, Neuilly Sur Seine, France, AGARD-CP-335, September 1982, pp. 14-1 to 14-14.

(A82-42813)

16. Abstract

A new method for computing the wall effects gives precise answers to some questions arising in adaptive wall concept applications: length of adapted regions, fairings with up- and downstream regions, residual misadjustments effects, reference conditions. The acceleration of the iterative process convergence and the development of an efficient technology used in CERT T2 wind tunnels give in a single run the required test conditions. Samples taken from CAST 7 tests demonstrate the efficiency of the whole process to obtain significant results with considerations of tridimensional case extension.

17. Key Words (Selected by Author(s))	18. Distribution Statement
	"Unclassified-Unlimited"

19. Security Classif. (of this report)	20. Security Classif. (of this page)	21. No. of Pages	22.
"Unclassified"	"Unclassified"		

USE OF ADAPTIVE WALLS IN 2D TESTS

J. P. Archambaud* and J. P. Chevallier
Office National d'Etudes et de Recherches Aérospatiales (ONERA)
*Research Engineer-ONERA-CERT, 31055 TOULOUSE CEDEX, FRANCE

Summary

A new method for computing the wall effects gives precise answers /1** to some questions arising in adaptive wall concept applications: length of adapted regions, fairings with up- and downstream regions, residual misadjustments effects, reference conditions. The acceleration of the iterative process convergence and the development of an efficient technology used in CERT T2 wind tunnels give in a single run the required test conditions. Samples taken from CAST 7 tests demonstrate the efficiency of the whole process to obtain significant results with consideration of tridimensional case extension.

Notations

C	integration constant
$f(\xi), g(\xi)$	auxiliary functions defined by (5) and (12)
c_{x_p}	pressure drag coefficient
c_{x_f}	pressure friction coefficent
c_{x_t}	total pressure coefficient (wash)
M	Mach number
p	pressure
p_i	generator pressure
T_i	generator temperature
h	section height
u, v	components of perturbation field on control surface near walls u_p, v_p, measured $u = \frac{\partial \varphi}{\partial x}$ $v = \frac{\partial \varphi}{\partial y}$
x, y	longitudinal and vertical coordinates in 2D section
β	compressibility factor $\beta = \sqrt{1 - m_0^2}$
φ	perturbation potential of confined flow
φ_m	perturbation potential due to model in unlimited flow
φ_i	interaction potential due to walls
ξ	integration variable following x
$\bar{\omega}, \omega^*$	reduction factor, optimum value

*Numbers in the margin indicate pagination in the foreign text.

Indices /2

B,H	lower walls, height
c	calculated by resolution of external displacement flow
d,i	direct method (shape given), inverse (velocity given)
p	wall
l,I	paired and unpaired parts
o	infinite upstream flow
ref	reference

Introduction

Minimizing wall effects of wind tunnels by giving to the streamlines which mark the boundary of the test section a shape identical to that which they would take at the same distance from the model with unlimited flow, is an idea which goes back at least 40 years [1].

It has undergone a very strong resurgence of interest in the last ten years thanks to consideration of external displacement ranges extending that of the wind tunnel up to infinity [2, 3, 4], and with which calculation allow us to ensure that the components of perturbation measured in the vicinity of the walls in the presence of the model correspond well to this flow. Published at the time where development of means and methods of calculation made it applicable [5, 6, 7], this concept has given rise to various choices of the mode of action on the transverse component of the flow, selection often dictated by concern for conserving in part existing installations [8, 9]. Nevertheless, while problems inherent with each type of wall present themselves (flexible [6, 7], perforated [7, 9] or slotted [8] walls), the same general questions must be dealt with for all solutions:

a) What length to give to the adapted section portion so that, with respect to the model, connections with the collector and diffuser produce only negligible perturbations?

b) How, with a section whose deformations prohibit recourse to standard vacuum displacement testings, to find precise reference conditions of velocity, in modulus and direction?

c) What are the residual wall effects connected to the inevitable adaptation defects?

d) How to accelerate convergence of adaptation processes to reduce residual corrections to tolerable levels without burdening the cost of

tests by a very large number of iterations.

Such are the questions which the works pursued at ONERA, after initial tests on a pilot installation [6], should allow us to respond to, in order to give complete effectiveness to a new wind tunnel installed at CERT [10].

Their outcome was thus undertaken within the framework of two groups of work: GART AG02 concerned with "2D transonic test methods", whose activity was made the object of a special report [37], and AGARD "Transonic Test Section" group [12].

Development of a method of calculation of wall effects [11] effectively using the components of perturbation measured on a control surface close to the section limits, and applicable from this fact regardless of the conditions at the limits, produces a clear response to the first three questions. It will therefore be reported straight away. Standard description of corrections in terms of velocity, incidence and their gradients, as well as considerations of symmetry, lead us to distinguish four boundary limits in modelling of streamlines. Separation of these boundary limits facilitates optimization of reduction factors to accelerate convergence of adaptation precesses.

Application of the principles thus developed can not be made without appropriate technology, which therefore will be described before demonstrating by several examples the total efficiency of the system. Taking into account these examples, and from the orders of magnitude expected, we also propose a possible extension of the process to tridimensional flows.

1. New Methods of Calculation of Wall Effects

1.1 Generalities

Calculation of residual corrections in a section approximately adapted to avoid blockage of the flow can allow us, following an idea of M. Carrière, to save the time of supplementary tests required to perfect its adaptation and the complicated and costly devices to per-

fectly model all the walls. On the other hand, development of new methods was encouraged by recommendations of the working group constituted at the initiative of AGARD [12]. They place in doubt the validity of conditions at the limits ordinarily admitted by ventilated walls and tempts us to use the distributions of pressure measured at the walls in the calculation of corrections. Following different routes, several authors have developed such methods almost simultaneously: Mokry, Peake, and Bowker [13] have introduced effective coefficients of porosity based on measurements of wall pressure. Methods with special features have been developed by Kemp [14], Smith [16], Hackett and Wilsden [19], and Blackwell [20]. C. F. Lo [17], on one hand, and Mokry and Ohman [18], on the other hand, have relied on Fourier transformations. Sawada [21] has developed a perturbation potential satisfying the equaiton for small transonic perturbations, in a series of functions of the components of perturbation measured on a control surface. Bringing about withdrawal, little justified it must be added, of an integral term and by retaining the standard hypothesis of an inherent field of the model identical to that which was present in infinite flow, it has expressed the correction of units of velocity as a function of deflections of the flow and corrections of incidence as a function of distributions of velocity. These integral expressions do not display the decrease of effects as a funciton of the distance to the model, which is why, with the objective investigated here, the method of Capelier et al. [11] appears to be preferable. It explains, as Sawada has previously done [22, 23], the influence functions used.

1.2 Report of Formulation of the Method of Signatures

The hypothesized principles are, as with standard methods, the following:

-subsonic compressible flow, assimilated by the Glauert rule to an incompressible flow whose perturbation velocities derive from a potential φ;

-breakdown of the potential into two terms φ_m and φ_i, corresponding respectively to the model and wall effects:

$$\varphi_i = \varphi - \varphi_m \qquad (1)$$

The potential φ_m corresponds to unlimited flow around a model presenting the same representative special features as the model submitted to perturbed field φ_i. Consequently, the interaction potential of the walls φ_i does not present any special feature between the limits of the jet stream. Determination of potential φ_i is carried out thanks to the following conditions: /3

-φ_i satisfies the potential equation

$$\beta^2 \frac{\partial^2 \varphi}{\partial x^2} + \frac{\partial^2 \varphi}{\partial y^2} = 0 \qquad (2);$$

-φ_i is continuous at the inside of a control surface constituted of two close parallel wall planes;

-the equations

$$\frac{\partial \varphi_i}{\partial x} = \frac{\partial \varphi}{\partial x} - \frac{\partial \varphi_m}{\partial x} \qquad (3)$$

and

$$\frac{\partial \varphi_i}{\partial y} = \frac{\partial \varphi}{\partial y} - \frac{\partial \varphi_m}{\partial y} \qquad (4)$$

are known on each of these planes since $\frac{\partial \varphi_m}{\partial x}$ and $\frac{\partial \varphi_m}{\partial y}$ are given by measurements carried out on the model and $\frac{\partial \varphi}{\partial x}$ and $\frac{\partial \varphi}{\partial y}$ by measurements carried out on the control surface.

Solution of the problem, by congruent transformation, is given in the appendix of reference [11] in the case where only $\partial\varphi/\partial x$ is known on the control surface. Corrections of velocity and incidence correspond to interaction potential φ_i. By assuming:

$$f(\xi) = \frac{\partial \varphi}{\partial x}(\xi) - \frac{\partial \varphi_m}{\partial x}(\xi) \qquad (5)$$

on the control surfaces with f_B for the lower wall and f_H for the upper wall, we discover on the axis of the section:

$$\frac{\partial \varphi_i}{\partial x}(x) = \frac{1}{\beta h} \int_{-\infty}^{\infty} \frac{f_B(\xi) + f_H(\xi)}{2 \operatorname{ch} \frac{\pi(\xi - x)}{\beta h}} d\xi \qquad (6)$$

$$\frac{\partial \varphi_i}{\partial y}(x) = \frac{1}{h} \int_{-\infty}^{\infty} \frac{f_H(\xi) - f_B(\xi)}{e^{2\pi \frac{(\xi - x)}{\beta h}} + 1} d\xi + C \qquad (7)$$

and for corrections of gradient and curvature:

$$\frac{\partial^2 \varphi_i}{\partial x^2}(x) = \frac{\pi}{\beta^2 h^2} \int_{-\infty}^{\infty} \frac{f_B(\xi) + f_H(\xi)}{2\, Ch^2 \pi(\xi - x)/\beta h}\, d\xi \qquad (8)$$

$$\frac{\partial^2 \varphi_i}{\partial y^2}(x) = \frac{2\pi}{\beta h^2} \int_{-\infty}^{\infty} \frac{f_H(\xi) - f_B(\xi)}{\left[e^{\frac{2\pi(\xi - x)}{\beta h}} + 1 \right]^2}\, d\xi \qquad (9)$$

Use of these formulas raises two difficulties:
a) f_B and f_H are expressed as a function of $\partial\varphi/\partial x$, perturbation potential, which assumes that we already know the velocity of the free stream which, indeed, will only occur after application of the correction.
b) the infinite limits of the integrals requires extrapolation of functions f_B and f_H which can be even more uncertain when they depend on the value selected for free stream.

Concerning the effect of initial systematic error δV_o on the uncorrected value of velocity attributed to free stream, we find that local velocities of perturbation are distorted by $-\delta V_o$. Introduced in functions f_B and f_H, they give a supplementary corrective term:

$$\delta\left(\frac{\partial \varphi_i}{\partial x}\right) = \frac{1}{\beta h} \int_{-\infty}^{\infty} \frac{-2\,\delta V_o}{2\, Ch \frac{\pi \xi}{\beta h}}\, d\xi \qquad (10)$$

By assuming $\lambda = \frac{\pi \xi}{\beta h}$ $\quad d\xi = \frac{\beta h}{\pi} d\lambda$, (10) becomes:

$$\delta\left(\frac{\partial \varphi_i}{\partial x}\right) = \frac{-\delta V_o}{\pi} \int_{-\infty}^{\infty} \frac{d\lambda}{Ch\lambda} = -\delta V_o \qquad (11)$$

This supplementary corrective term exactly offsets the initial error δV_o.

The second difficulty concerning extrapolation of functions f_B and f_H can be avoided by bringing about truncation of the integrals, reducing for example the limits to the effective length of the test section.

The error thus introduced is completely negligible from the fact that in formulas (1) and (3) functions f_B and f_H are limited (and also approach zero for $\xi \to \infty$), and that the function $ch\,\pi(\xi-x)/\beta\ell$, which appears in the denominator, increases very rapidly with ξ and which loses all significance at the remote regions of the model. This remark validates the preceding for a section of finite lenght. Representation of the influence function (figure 1) concerning veleocitites furthermore demonstrates that the region on which it is necessary to know f_B and f_H decreases when the Mach number increases.

Within the framework of linear approximation, the preponderant zone of influence also approaches zero when the Mach number approaches one; this limit does not have a physical sense since it would be advisable at least to extend to the line of the profile the average of the Mach numbers corrected on the axis. But we can at once conclude that the measurements of wall speed carried out on three half-lengths of the section from one part to another of the model suffice to determine without appreciable error reference speeds greater than M=0.3.

Equation (2), which gives the incidence correction, does not present the same advantages: the influence function approaches one for the upstream region, thus protected in so far as the reference, and it is necessary that the section be sufficiently long so that $f_B - f_H$ effectively approaches zero. From the practical point of view, this does not avoid a certain uncertainty which we can estimate from equation (2). For a vacuum section, the difference of velocities between floor and ceiling, assumed constant and integrated on a length equal to the height of the section, gives the order of magnitude $\Delta \propto \overline{\overline{u_H - u_B}}$. In order to know the incidence to a few hundredths of a degree, it would be necessary to know u_H and u_B to approximately 1/2000. /4

To escape from these difficulties, recalling the demonstration of equations (1) to (4) given by [11], we no longer assume knowledge of the real portion of the complex potential, but its imaginary portion. By assuming:

$$g(\xi) = \frac{\partial \varphi}{\partial y} - \frac{\partial \psi_m}{\partial y} \qquad (12)$$

Paquet [15] resorts to a combined formulation which gives in particular on the axis:

$$\frac{\partial \varphi_i}{\partial y}(x) = \frac{1}{\beta R}\int_{-\infty}^{\infty} \frac{g_1(\xi) + g_2(\xi)}{2\,\mathrm{Ch}\,\pi(\xi - x)/\beta R}\,d\xi \qquad (13)$$

the integration constant appeared when in the expression of $\varphi_i/\partial x$ and expression (13) presents for determination of incidence the same advantages of (6) for calculation of velocity. It demonstrates that the wind direction at emplacement of the model, deduction made from the model boundary limit, is a means of losses of flow on the control surface balanced for one function, decreasing very rapidly with the distance from the model (figure 1). It can thus be applied without harm with truncation of the integration limits. Initial error on the reference from which the losses of flow are measured thus finds itself corrected automatically.

The precision required on measurements of loss is no grater than that which we investigate for the wind direction and we can, if angular measurements are carried out on a great number of points of the control surface, benefit from the statistical effect of numerous independent measurements.

Equations (6) and (13) therefore present decisive advantages of principle for determination of the Mach number and reference direction of the flow. Their application nevertheless collides with normal practices and runs into the following difficulties:

a) as with standard methods, representation of the model by special features is necessary and it becomes difficult in the transonic range where the limit of application is not obvious;

b) precise measurements of the direction of the flow are, in spite of the works of Wittliff or Bodapati et al. [24], even more delicate than measurements of velocity in the vicinity of permeable walls.

We will see later that these difficulties can be circumvented and will only delay, for adaptable sections, a conclusion whose validity exceeds the framework of the hypotheses used to explain the influence

functions of (6) and (13). Reference velocity and direction of the flow at emplacement of the model only depends respectively on the velocities and directions measured on a control surface near the limits of the section with influence decreasing rapidly toward upstream and toward downstream.

2. Wall Adaptation Processes

Before describing in detail the technology used to shape the solid and flexible walls used at T2, retained to expose the principle of their adaptation, we arrangenumerous collections of wall pressures and measurements of displacement giving distributions $p_{p_i}(x)$ and $y_p(x)$, and rapid calculation of limit layer, based on pressures measured, which allow us to correct $y_{p(x)}$, thicknesses of displacement, in order to understand the shape of streamlines limiting the flow of perfect fluids.

The principle of adaptation, stated many times [2, 3, 4, 5, 6, 7, 8, 9, 13, 24, ...], calls for attention to resolution, in the virtually unlimited range without special features, of a problem relating to data on the control surface plane near the wall, either measured longitudinal perturbaiton velocities u_p deduced from pressures, or transversal perturbaiton velocities v_p corresponding to losses $-\partial y_p/\partial x(x)$.

Solutions (by Green function, or numerical methods) furnish respectively v_e or u_e and adaptation will be obtained when simultaneously:

$$\begin{aligned} u_p(x) &= u_e(x) \\ v_e(x) &= v_p(x) \end{aligned} \qquad \forall x \qquad (14)$$

If we have taken u_p as given information, the virtual field calculation gives v_c and the comparison will bear on the equality $v_c = v_p$?, since condition $u_c = u_p$ is accomplished at the start. If $v_c \neq v_p$, we will attempt to improve adaptation by reduction processes in which a linear form of v_c and v_p can furnish an improved value:

$$v_a(x) = \omega_i v_c(x) + (1-\omega_i) v_p(x) \qquad (15)$$

Are these processes convergent? How to select the reduction fac-

tor to obtain rapid convergence? Does convergence ensure validity of the solution obtained? We will not deal with this last question, demonstration of existence and unicity being given by Ciavaldini [30].

The response to the first question is not obvious: Sears finds that the most convincing study rests in numerical simulation of the set of processes [25], since purely analytical studies limit themselves to rather simple classes of models and wind tunnels [26, 27]; it nevertheless studies the effects of imperfections in control [28] which do not preclude convergence toward an imperfect, but better than before repetition, solution.

Our own experiment [6] with a reduction coefficient of 0.5, that is to say approximately that of optimum values proposed later on [26, 27], has demonstrated that divergence could appear when the sensitivities of external and internal flows at a variation of v are very different. This possibility has also been pointed out by Judd et al. [29]. /5

Sensitivity of the internal flow to variations of v is, due to the law of high subsonic atmospheres,much more significant than that of external flow. It is clear that if in this case we are afraid of divergence with a reduction coefficient of 0.5, we can also select it to ensure stability, but at the price of a greater number of repetitions. Indeed, a well-chosen value of the reduction coefficient would lead in a single stage to adaptation [27], but this value can depend closely on the flow of the model: in strong interaction regime between limit layer and shock wave, a weak longitudinal gradient of the Mach number modifies position of shock, separation, C_x, and thickness of the wash. To optimize selection of the reduction mode, it appeared interesting to analyze the shapes of sections by describing them not by immediate data $y_u(x)$ and $y_d(x)$, but in terms of height of section $h(x) = y_u - y_d$ and median line $m(x) = (y_u + y_d)/2$, and considering for each of these functions decomposition into paired and unpaired parts:

$$h_p(\pm x) = (h(x) + h(-x))/2 \qquad h_i(x) = -h_i(-x) = (h(x) - h(-x))/2$$
$$m_p(\pm x) = (m(x) + m(-x))/2 \qquad m_i(x) = -m_i(-x) = (m(x) - m(-x))/2 \qquad (16)$$

For sections of simple shapes, these functions correspond repectively to enlargement of the section at its divergence, at the camber of its mean line and at the adjustment of this in relation to the horizontal. We can associate these terms with effects induced by volume of the model, its wash, its lift, and the reference incidence. Sensitivity of internal and external flows to variations of camber of the mean line is very close and the analysis of Lo and Kraft can be applied [27]. For the adjustment, at the inverse of divergence, the sensitivity of external flow is evidently greater than that of internal flow. We will see in applications that it is not necessary to determine partial factors with great precision to obtain completely satisfactory convergence.

3. Remarks

3.1

The preceding considerations on the contribution of the new method of calculation of wall effects with the use of a section provided with an active control device of transversal flow are general applications, whatever the type of wall. We have nevertheless demonstrated the necessity, in order to determine with precision the reference direction of the flow, of resorting to measurements of the same nature on all of the control surfaces to obtain a significant weighted average. Although this motive had not been at the origin of selection of the solution retained (movable solid wall) for wind tunnel T2, it appears "a posteriori" that this was the single one which could provide knowledge of the direction of the flow with the precision required, without supplementary devices (probes, laser, ...), and with the minimum of time.

3.2

To simplify acquisition of reference conditions within a section which, without being perfectly adapted, nevertheless approaches this condition, we have proposed [31] concerning the velocity standard for calculating the virtual external flow for the shape given of the running layer as a function of the velocity at infinity and of selecting this to minimize the balanced distances between local calculated and measured velocities. The function of initially proposed balancing was the squared inverse of the distance to the center of the section.

Taking into account analysis of residual corrections, it is consistent to adopt for balancing the function $1/(\mathrm{ch}\ \pi(\xi-x)/\beta h)$ which appears in equation (6) for correction of velocity.

We put this into words to make apparent the terms providing measurements at the wall and from the field of the model:

$$\frac{\partial \varphi_i(x)}{\partial x} = \frac{1}{\beta h}\int_{-\infty}^{\infty} \frac{\left[\left(\frac{\partial \varphi}{\partial x}(\xi)\right)_M + \left(\frac{\partial \varphi}{\partial x}(\xi)\right)_B\right]_f - \left[\left(\frac{\partial \varphi}{\partial x}(\xi)\right)_M + \left(\frac{\partial \varphi}{\partial x}(\xi)\right)_B\right]_r}{\mathrm{ch}\ \pi\frac{\xi - x}{\beta h}} d\xi \qquad (17)$$

the second bracket, index m, represents in unlimited flows overspeeding due to the model on the control surface. These are by definition identical to those which we would obtain in the presence of perfect adaptation of the confined section. If we assume the existence of an optimum reduction factor $\overline{\omega}^*$ defining this distribution from elements measured (indices f) and calculated (indices c) for the preceding stage; we have:

$$\left[\frac{\partial \varphi}{\partial x}(\xi)\right]_m = \overline{\omega}^*\left(\frac{\partial \varphi}{\partial x}\right)_c + (1-\overline{\omega}^*)\left(\frac{\partial \varphi}{\partial x}\right)_f \qquad (18)$$

which placed in the preceding formula gives:

$$\frac{\partial \varphi_i(x)}{\partial x} = \frac{\overline{\omega}^*}{2\beta h}\int_{-\infty}^{\infty} \frac{\left[\left(\frac{\partial \varphi}{\partial x}(\xi)\right)_M + \left(\frac{\partial \varphi}{\partial x}(\xi)\right)_B\right]_f - \left[\left(\frac{\partial \varphi}{\partial x}(\xi)\right)_M + \left(\frac{\partial \varphi}{\partial x}(\xi)\right)_B\right]_c}{\mathrm{ch}\left(\pi(\xi-x)/\beta h\right)} d\xi \qquad (19)$$

If we select the reference velocity so that the weighted averages of calculated and measured distributions of $\frac{\partial \varphi}{\partial x}(\xi)$ are equal, velocity correction is nil. We have thus, even though the adaptation is not perfect, a consistent definition of the reference velocity with the method of calculation of wall effects and which does not require recourse to representation of the model nor to knowledge of $\overline{\omega}^*$.

The same demonstration applies to determination of the reference direction by substituting magnitudes of the same nature. Established from hypotheses allowing linearization, it nevertheless preserves a physical sense when M apporaches 1 at conditions leaving the balancing function, becoming very "sharp-pointed". Another incentive for en-

larging the preponderant influence zone of the wall comes from extension of the model for which not only the velocity at the section center, but a certain average length of the line, is significant. Practically, neglect of the compressibility factor β can constitute an acceptable solution. /6

It is necessary to underline that knowledge of the standard reference velocity and direction defined with a section in adaptation route at best allows possible defects of curvature and divergence to exist.

3.3 Extension to Tridimensional Flows

The new method of calculation of wall effects [11] has been extended from the outset to periodic tridimensional flow corresponding to the test model with a rectangular section whose lateral walls remained solid and whose lower and upper walls can be more or less adapted [15].

To formulas established from distributions of pressure, we add, thanks to introduction of the direction measured of the flow, conjugated formulas which, as for two-dimensional flow, take the same self-corrective form, and justified by the presence of Ch functions in the denominators of the same truncated integrals.

On the other hand, we observe that the series expressing corrections as a function of harmonic decomposition of functions f and g(y) in the sense of the breadth of influence functions decreases very fast, as well as a function of χ of their range. We can deduce, taking into account the order of magnitude of corrections, that we should be able to propose, as a good first approximation, to operate in the following fashion.

The wind tunnel was equipped to ensure deformations of the two-dimensional walls in level streams, using the transversal method of measurements of wall velocity to ensure the adaptation which defined the Mach number and incidence and completely cancelled the longitudinal gradient and curvature defect. We calculate residual corrections due

due to model reflections in relation to the lateral walls and to transversal non-uniformity of the discharge following the new method.

The result will probably justify limiting it, if a narrower adaptation is revealed to be necessary, to relatively simple solutions such as those of Ganzer [32, 33] (octagonal section) or Whitfield et al. [34] (6 independent segments per wall).

3.4

The conclusions obtained on the weak influence of regions remote from the model at the upstream and downstream should not lead to confusion. The flow which approaches the adapted region thus must be as pure as possible: upstream filters, convergent designs and relationships with the adapted zone, wall angles, supports and lateral limit layers, must be dealt with to avoid introduction of extraneous secondary flows which did not at all eliminate wall adaptations.

4. Description of Methods Displayed

4.1 T2 Wind Tunnel

The T2 wind tunnel is a 1/10 scale model of the project proposed by ONERA for construction of a large European transonic wind tunnel. It has functionned since 1975 [35].

It concerns an induction wind tunnel, formed by a closed circuit approximately 25 m long. It runs presently by cryogenics and use of deformable walls in this realm is envisioned in 1983. The circuit is pressurizable up to 5 bars; the Mach number ranges between 0.3 and 1.1. The intensity of turbulence in the test section is on the order of magnitude of 0.002. T2 runs by bursts of 30 to 60 s. At starting, preinflated circuits, stationary flow establishes itself in approximately 10 s.

Bend number 1 (figure 2) is equipped with bladings whose leakage side allows jets of air under pressure to escape (p_{ij}=7 b; M_j=1.6). These jets produce the fluid contained in the circuit, through a low velocity return portion, the plenum chamber (1.8x1.8 m^2), collector

(20 contraction ratio), section, collar, and finally a section of porous wall where partial evacuation occurs. The collar stabilizes discharge into the section and completely prevents resumption of perturbations issuing from evacuation and injection zones.

4.2 Test Section

The section is a significant element of the wind tunnel in this experimentation genre. For the present two-dimensional tests, this idea has been made the object of special attention in order to know as precisely as possible conditions at the boundaries of the range (geometric definition and pressure measurements) and to operate with precision on the walls.

This section has dimensions of L=1.32, m-1=0.39 m, h=0.37 m. It is formed by two fixed parallel vertical walls and by two flexible upper and lower walls of 1.5 mm thick sheet steel. Upstream, these deformable walls are screwed onto the end of the collector to accomplish continuity of gradient; on its longitudinal sides, teflon joints ensure air-tightness and slipping. Downstream, the vertical opening of the section, variable according to the test configurations, is extended by two movable valves connected to the collar (figure 3) to avoid sudden changes of profile.

Each flexible wall is deformed by 16 hydraulic jacks (basic step 0.2 mm; maximum travel 25 mm) operated by electric impulse motors. These jacks are closer together in the influence zone of the model. Each jack, through the intermediary of a system of low-play small rods (less than 1/10 mm), displaces identically two points of a transversal stiffeneer joined to the wall (figure 4). The small rod-stiffener connection is formed by a swivel-joint in order to avoid appearance of local moments of flexion. We have observed good transversal inherent flatness of the walls.

The sides of the deformable boundaries are adjusted by potentiometric comparators placed at right angles with the jacks (5/100 mm precision). The origins of measurement of these potentiometers corre- /7

sponds to a flat horizontal wall; in this position, manual adjustment of sides demonstrates some defects, negligible in the zone of the model, but more pronounced between the farther-apart jacks at the ends of the section; these bombardments of the wall, less than 3/10 mm, nevertheless reflect in visible fashion on the pressure adjustments (figure 5).

Each flexible wall is equipped with 91 pressure bleeds (ϕ=0.4 mm), narrower in the region of the model and distributed on 3 longitudinal generators.

4.3 Model

The results presented are relative to CAST 7 profile. This is a supercritical profile of 12% relative thickness, selected by the GART group with the objective of comparing various wind tunnels.

We have used 2 models of 120 and 200 mm of line, equipped respectively with 102 and 103 pressure bleeds of diameter ϕ=0.4 mm; each model can be placed at whatever position between the section axes and 80 mm underneath (20% of the section height).

The incidence of the model is manually adjusted to ± 1 in relation to the horizontal.

The transition is artificially triggered at 7% of the line on both faces by silicon carbide grains cemented on a band of 1 mm width. The reflection of grains has been defined from a criterion of triggering of the transition corresponding to a considerable extent to the displacement thickness of the laminar limit layer in front of the corrugation.

4.4 Measurements and Acquisition

Instrumentation of the wind tunnel, besides analogical pathways (pick-ups, enlargers), includes an HP 1000 computer and its peripherals. The various sequences are programmed by this computer, which ensures acquisition of data at the time at the rate of 1000 points/s (pressures, sides) and controls displacement of jacks; concurrently, it records the results acquired on a disc file.

All the pressure bleeds are consolidated on 7 "standard" scanivalve heads, each including 48 bleeds scanned at the rate of 10 bleeds per s; indeed, we measure $p - p_{ref}$ by differential pick-ups to have better precision.

The wash is joined with a line downstream of the leakage edge of the model by two static pressure bleeds and interdependent stop-valves of an exploration tip.

Analogic pressure and position data are converted into numerical values treated by calculation.

5. Test Development

A complete test for a given configuration requires 2 bursts; the first is devoted to auto-adaptation of the walls by iterative processes; the second is reserved for probing of the wash.

5.1 Wall Adaptations

We present here the series of operations required for wall adaptations; each phase will be detailed in the following paragraphs.

In a fashion to minimize the number of repetitions, we initially position the walls in a shape called initial, approaching as much as possible the affected result. With these conditions, adaptation is accomplished in absolute time by 3 to 5 repetitions which occur at the same burst. The computer runs only to execute the various operations.

Each repetition can be broken down as follow:

- -positioning of the walls: duration 1 s
- -pressure measurements on the walls and profile: duration 5 s
- -calculation of new wall shapes: duration 4 s

} 10 s

At the end of the bursts, it is possible to graph local Mach numbers and wall shapes for each repetition, and local Mach numbers and pressure coefficients on the profile; we can also integrate pressures on the profile to obtain C_x, C_z, C_m for each adaptation stage.

These results are very useful to define the convergence property; indeed, we fix the number of repetitions before the test; no convergence criterion interferes during the burst. Adaptation of the section is judged to be good when the distribution of the Mach numbers does not develop further from one repetition to the next; local oscillation between two neighboring jack positions (0.2 mm) can even exist.

5.2 Initial Shapes

We use two modes of investigation of initial shapes. Initially, we simply position the walls on an adapted geometry, result of a preceding test relative to a slightly different configuration: same boundless Mach number, varying incidences; same incidence, varying boundless Mach numbers.

The second solution is given by calculation of flow around special pinpoint features in boundless atmosphere, special features (source, doublet, vortex) whose intensities are approximately estimated from C_x, profile section, and C_y, which are placed at the center of the model. We deduce the shape from limited passage by steamlines issuing from the section entry, which we extend after calculation of wall limit layers. /8

Positioning of the walls in their initial shapes is carried out before the start of the burst. We then adjust the opening of the movable valves, at the entrance of the collar, on the downstream section of the section to avoid surface discontinuities. This adjustment is not altered during the test, but slight variation of the ends of the flexible walls during repetitions justifies this step.

5.3 Positioning of the Walls

At the start of each repetition, we ensure that the geometry realized is mechanically acceptable (test on local ray curvature). If it is not, we make an adjustment of the sides before deformation, then positioning is accomplished by stages on improved intermediary shapes; finally, a second adjustment of sides registers the shape actually obtained. At this time, non-compliance of displacement of a section in-

terrupts the test.

5.4 Calculation of New Shapes

The new shapes are defined by an inverse linear method: we assume $u_c(x) = u_f(x) = -u_\infty \frac{K_p}{2}$. The vertical velocity $v_c(x)$ in the external virtual field is calculated by Green method applied on a horizontal plane: $v_c(x) = \int_{-\infty}^{\infty} \frac{u_c(\xi)}{\xi - x} d\xi$. Finally, the new streamline is determined by integration from the section entry: $y(x) = y_{\text{entrée veine}} + \int_{x \text{ entrée veine}}^{x} \frac{v(\xi)}{V_\infty - u(\xi)} d\xi$. The difference between the old and new streamlines gives the displacement to impose on the wall.

Compensation for the effect of obstruction of 4 wall limit layers is reported on each of the flexible walls. Each of them balances its own limit layer (calculated from measured pressures) and that which exists on one of the two vertical doors (considered as plane plate at v_0). Calculations are carried out by an integral method [36] which uses as the starting point magnitudes of the turbulent limit layer probed at the end of the collector.

For a better reduction of the processes, pressures and sides measured are broken down into paired and unpaired portions of 2 functions connected to the height of the section and the median line (see end of chapter 2). It is therefore necessary to create a symmetrical calculated meshing in x. In the present case, we ficticiously lengthen the section toward downstream by adding virtual points. With this calculated meshing, each point is an average of several pressure bleeds. Decomposition of the calculation into 4 independent released portions separated besides the effects of volume (V), source (S), lift (P), and adjustment of average distortion (VDM). Vacuum section tests from initial shapes corresponding to each effect have allowed us to roughly optimize reduction coefficients; they depend little on the Mach number. For our tests we have retained the following values:

incidence		- 2°$\dot{\alpha}$ - 1°	0°$\dot{\alpha}$ + 5°
ω_1	V	0.3	0.2
	S	0.2	0.2
	P	0.6	0.4
	VDM	0.6	0.6

In the calculation of the virtual external field by the Green method, integration of u on the horizontal boundless control surface is broken down into three parts:

$$v_e(x) = \int_{-\infty}^{\infty} \frac{u(\xi)}{\xi - x}\, d\xi = \int_{-\infty}^{\text{section entry}} + \int_{\text{entry}}^{\text{exit}} + \int_{\text{section exit}}^{+\infty}$$

The central term corresponds to the extended section and can interfere with pressure measurements. The outside terms are estimated for volume, source, and lift effects by analytical integration of expression $u(\xi)/(\xi - x)$ relative to the respective special features; moreover, it allows us to use this modeling for estimation of the model field with second order terms, although the adaptation method claims, as a principal advantage, of being able to result from this representation.

6. Typical Results

6.1 Standard Adaptation Case

The example corresponds to the model of 120 mm line, placed on the section axis, at 1° incidence, M_o=0.70. At the start, divergence of the walls balances only the limit layers (figure 5); the streamlines limiting the range of perfect fluid are thus approximately parallel. In this flat wall canal and for this upright case, the velocity attains higher values on the upper wall (M=0.8). From the second repetition, this maximum decreases and the general aspect of distributions of velocity is attained. The third repetition improves adaptation and the fourth confirms the result at a nearby section step (0.2 mm).

We can observe oscillatory type convergence of the processes con- /9

nected to the reduction coefficients selected and the rapidity of this in spite of initial geometry of extended walls of the adapted shape.

On the model, adaptation, by releasing the discharge, makes the shock advance more then 10% of the line and lowers the general level on 2 faces (figure 6).

6.2 Influence of Position of Model in Section

Theoretically, vertical displacement of the model within the frame of reference of the section must produce a different adaptation of the walls without modifying the field of pressures on the profile. This constitutes an intrinsic test of the complete processes whose approximations are not necessarily completely justified.

This test has been carried out at T2, in the configuration M_o= 0.76, α=1, profile of 120 mm of line. The model has been placed on the section axis some 80 mm underneath (20% of the height of the section entry) (figure 7).

We can state that lowering of the model, in this upright case, has extended the upper demi-canal by decreasing overspeeding at the upper wall. This result is appreciable when we approach the limits of validity of the calculation hypothesis, especially linear formulation for local Mach numbers near 1.

On the profile and with the wash, we distinguish slight differences (figure 8).

6.3 Angle of Incidence

The problem of the angle of incidence of the model in a flow of finite length has been developed in the preceding portions.

Experimentally, we have displaced adapted walls (M_o=0.70; α=1°) by simple rotation around the section entry at an angle of $\Delta\alpha=\pm 0.18°$. In both cases, the walls are approximately adapted.

We can see on figure 9 that values of α corresponding to these tests are in good agreement with the general curve $C_{\gamma(\alpha)}$ obtained by making the profile rotate. This result allow us to conclude that:
-change of collector-section connection to a negligible influence at the level of the model;
-reference direction of free stream is well defined for wall loss in the vicinity of the model.

6.4 Longitudinal Velocity Gradient

In order to test the possibility of applying a correction of longitudinal velocity gradient, systematic variation of divergence of the section has been accomplished by making the adapted shapes pivot (figure 10a), as previously. The pressure drag coefficient is shown on figure 10b as a function of this divergence, to which a static longitudinal pressure gradient corresponds. Standard correction of Archimedes thrust gives in this case (M=0.70, profile of 120 mm of line) an obviously lower gradient than which development stated for a flow decelerated by divergence of the section.

6.5 Actual Possibilities of Installation

Figure 11 gathers the different flexible wall shapes obtained after adaptation around the model of 200 mm of line placed in basic position; the boundless Mach number goes to 0.70; incidence varies between -2° and $+4^{\circ}$; we observe regular development of shapes between -2° and $+2^{\circ}$, then deceleration of this development ($\alpha=3^{\circ}$) to approach the maximum value of C_{γ} following significant downstream widening of the section ($\alpha=4^{\circ}$) corresponding to the rough increase of drag.

Conclusions

In relation to the questions underlined in the introduction, practical use of adaptable walls in the T2 wind tunnel for profile tests allows us to give the following responses:
a) taking into account the rapid decrease, with the distance from the model, of the influence function of adaptation defects, the length of adaptable walls selected for T2 appeared sufficient and with these con-

ditions the connections of the collector and downstream collar are without significance;

b) although, with respect for gain of time, precise conditions at infinity have not been investigated in the present tests by reference to the set of wall measurements, some controls [38] have demonstrated that the differences were on the order of measurement errors;

c) on the other hand, it appeared that the step selected (0.2 mm) for displacement of the walls can also allow a non-negligible camber defect (0.2^{o}) to exist for a profile of sufficiently large line, in relation to the precision required in definition of the profile;

d) separation into four boundary limits according to symmetries allows us, by appropriate selection of constant reduction coefficients, to sufficiently accelerate convergence of the adaptation processes so that a single burst suffices to attain the adjustment threshold. Increase of the test cost thus corresponds to doubling of the time since another burst is currently necessary for acquisition of the measurements (wash and pressure) on the profile.

Outside these responses to the initial questions, the possibilities offered to carry out these tests without adaptation have allowed us to test methods of calculation of corrections and also to put to the test, concerning the longitudinal velocity gradient, the validity of the drag correction.

There remains at high Mach numbers uncertainties on the possibility of applying in the presence of non-linear effects corrections connected to non-uniform perturbations (camber and velocity gradient), this leads us to conclude that the price paid for sufficient adaptation to conditions at the limits and precise knowledge of references must be accepted when precise results are investigated. /10

REFERENCES

1. Lock, C.N.H. and J.A. Beavan, "Tunnel interference at compressibility speeds using the flexible walls of the rectangular high-speed tunnel",ARC R and M 2005 (1944).

2. Ferri, A. and P. Baronti, "A method for transonic wind tunnel corrections", AIAA Journal 11/1, 63-66 (January 1973).

3. Sears, W.R., "Self correcting wind tunnels", Aer. Journ. 78/758-759 (February-March 1974).

4. Legendre, R., "Self correcting transonic wind tunnels", Ommagio a Carlo Ferrari Lib. Leurotto et Bella Turin, pp. 457 (1974) and Onera, T.P., pp. 33 (1975).

5. Vidal, R.J., J.C. Erickson, and P.A. Catlin, "Experiments with a selfcorrecting wind tunnel", AGARD CP 174, Paper no. 11, October 1975.

6. Chevallier, J.P., "Transonic wind tunnel with self correcting walls", AGARD CP 174, Paper No. 12, October 1975.

7. Goodyer, H.J., "A low speed self streamlining wind tunnel", AGARD CP 174, Paper no. 13, October 1975.

8. Weeks, T.M., "Reduction of transonic slotted wall interference by means of slat contouring", AFFDL TR 74-139, 1976.

9. Kraft, E.M. and R.L. Parker, "Experiments for the reduction of wind tunnel interference by adaptive wall technology", AEDC TR 79-51, October 1979.

10. Quemard, C. and A. Mignosi, "Definition of a high quality induction wind tunnel from the pressurized transonic T2 wind tunnel of ONERA-CERT",Eighteenth Israeli Conf., Haifa, May 19, 1976.

11. Capelier, C., J.P. Chevallier, and F. Bouniol, "New method of correction of the effects of two-dimensional walls", Fourteenth Aerodynamic Symposium Report 21, Toulouse, November 1977 and R.A. no. 1, pp. 1-11, 1978.

12. Pindzola, M., J.W. Binton, and J.P. Chevallier, "Comments on wall interference control and corrections", AGARD CP 187, April 1976.

13. Mokry, J.M., D.J. Peake, and A.J. Bowker, "Wall interference on two-dimensional supercritical airfoils using wall pressure measurements to determine the porosity factors for tunnel floor and ceiling",NAE NRCC Ottawa, Aer. Rep. 4-R-574, February 1974.

14. Kemp, W.B., "Toward the correctable interference transonic wind tunnel", Ninth AIAA Aer. Testing Conf.,June, 1976.

15. Paquet, J.B., "Perturbations induced by the walls of a wind tunnel", Ing. Doc. Thesis, Lille, June 26, 1979.

16. Smith, J., "Preliminary evaluation of a method for determining 2 dim. wall interference", NLR Memo AC 77-008, March 1977.

17. Lo, C.F., "Tunnel interference assessment by boundary measurements", AIAA Journ. 16/4, 4-413 (April 1978).

18. Mokry, M. and L.H. Ohmar, "Application of the fast Fourier transform to this dimensional tunnel wall interference", J. of Aircraft 17/6, (June 1980).

19. Hackett, J.E. and D.J. Wilsden, "Estimation of wind tunnel blockage from wall pressure signatures: a review of recent work at Lockheed Georgia",AIAA. Rep. 78-828.

20. Blackwell, J.A., "Wind tunnel blockage correction for two-dimensional transonic flow", J. Aircraft 16/4, 256-2 (April 1979) and AIAA Pap. 78-805.

21. Sawada, H., "A general correction method of the interference in 2-dimensional wind tunnels with ventilated walls.

22. Sawada, H. et al., "An experiment of lift interference on 2 dimensional wings in a wind tunnel with perforated walls", N.A.L. T.R. 563, March 1979.

23. Sawada, H., "Experimental study about 2-dimensional blockage effect", N.A.L. T.R. 591, November 1979.

24. Bodapati, S., E. Schairer, and P. Davis, "Adaptive wall wind tunnel development for transsonic testing", AIAA Pap. 80.0441.

25. Sears, W.R., R.J. Vidal, J.E. Erickson, and A. Ritter, "Interference free wind tunnel flows by adaptive wall technology", J. of Aircraft 14/11, 1042-1050 (November 1977).

26. Sears, W.R., "A note on adaptive wall wind tunnels", ZAMP 28, 915-927 (1977).

27. Lo, C.F. and E.M. Kraft, "Convergence of the adaptive wall wind tunnel", AIAA Journ. 16, 67-72 (January 1978).

28. Sears, W.R., "Adaptive wind tunnels with imperfect control", J. of Aircraft 16/5, 344-3-8, art. 79-4072 (June 1978).

29. Judd, M., M.J. Goodyer, and J.W. Wolf, "Application of the computer for on site definition and control of wind tunnel shape for minimum boundary interference", AGARD CP 210, Pap. no. 6 (June 1976).

30. Ciavaldini, J.C., "Numerical analysis of compressible flows around a profile placed in boundless atmosphere", Doctoral Thesis, Rennes, Oct. 17, 1980.

31. Gely, J.M., "Self adaptation and corrections of transonic wind tunnel walls", Ing. Doc. Thesis, Toulouse, September 27, 1979.

32. Ganzer, U., "Wind tunnels with adapted walls for reducing wall interference", A. Flugwiss Weltraumforsch 3, 129-133 (March-April 1979).

33. Ganzer, U., "Adaptable wind tunnel walls for 2D and 3D model tests", ICAS Conf. Pap. 23.3, Munich, 1980.

34. Whitfield, J.D., J.L. Jacocks, W.E. Dietz, and S.R. Pate, "Demonstration of the adaptive wall concept applied to an automotive wind tunnel", AIAA Twelfth Aer. Test. Conf., March 1982.

35. Mignosi, A. and C. Quemard, "Performances and flow qualities of the T2 induction wind tunnel", La Recherche Aérospatiale 1976-4.

36. Michel, R., C. Quemard, and J. Cousteix, "Practical method for anticipation of the two- and tridimensional turbulent limit layers", Applied Aerodynamics Symposium, AAAF, Saint-Louis, November 1971.

37. Elsenaar, A. and E. Stanewsky, "A report of a GARTEUR Action Group on "Two-dimensional Transonic Testing Methods"", AGARD Specialist Meeting, London, 1982.

38. Ashill, P.R. and D.J. Weeks, "A method for determining wall interference corrections in solid wall tunnels from measurements of static pressure at the walls", AGARD Specialist Meeting, London, 1982.

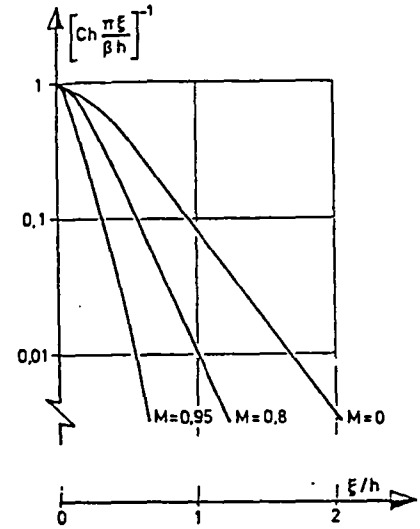

Figure 1. Function of influence balancing wall effects as a function of distance from the model according to the direction of the flow.

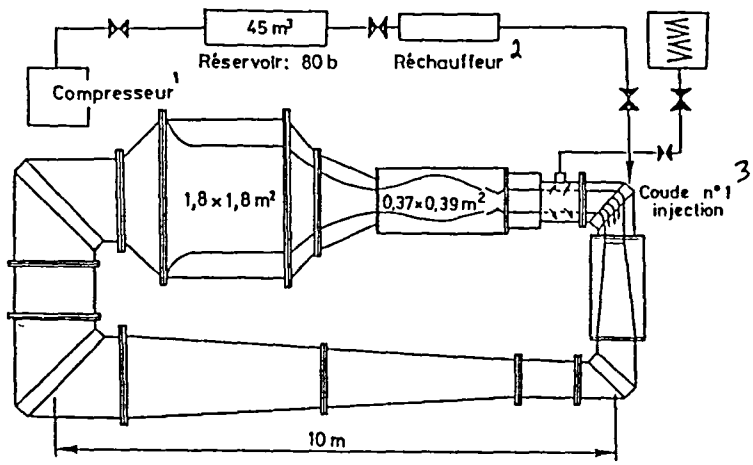

Figure 2. Diagram of the CERT T2 wind tunnel.

Key: 1-Compressor; 2-Reheater; 3-Bend no. 1.

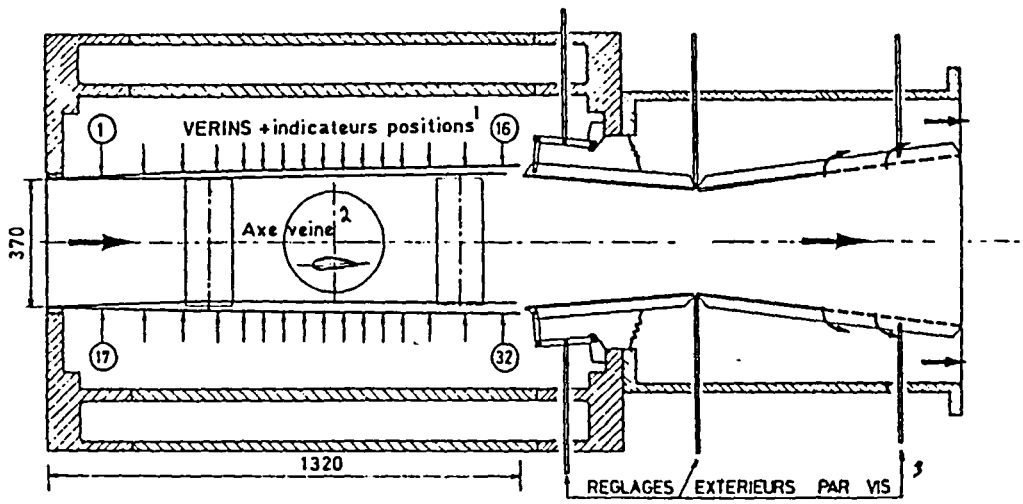

Figure 3. Deformable wall section.

Key: 1-Bleeds + position indicators; 2-Section axis; 3-Outside adjustment by screws.

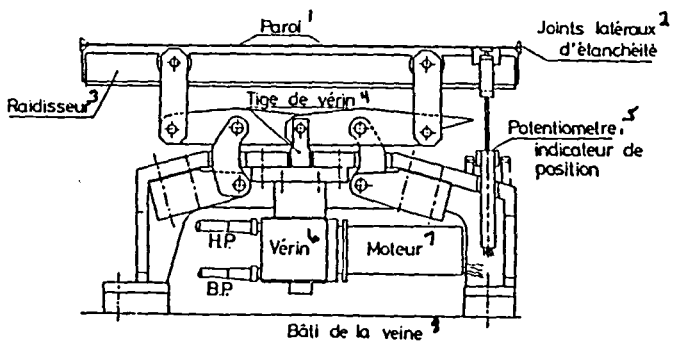

Figure 4.

Key: 1-Wall; 2-Lateral air-tight joints; 3-Stiffener; 4-Jack shaft; 5-Potentiometer, indicator of position; 6-Jack; 7-Motor; 8-Frame of the section.

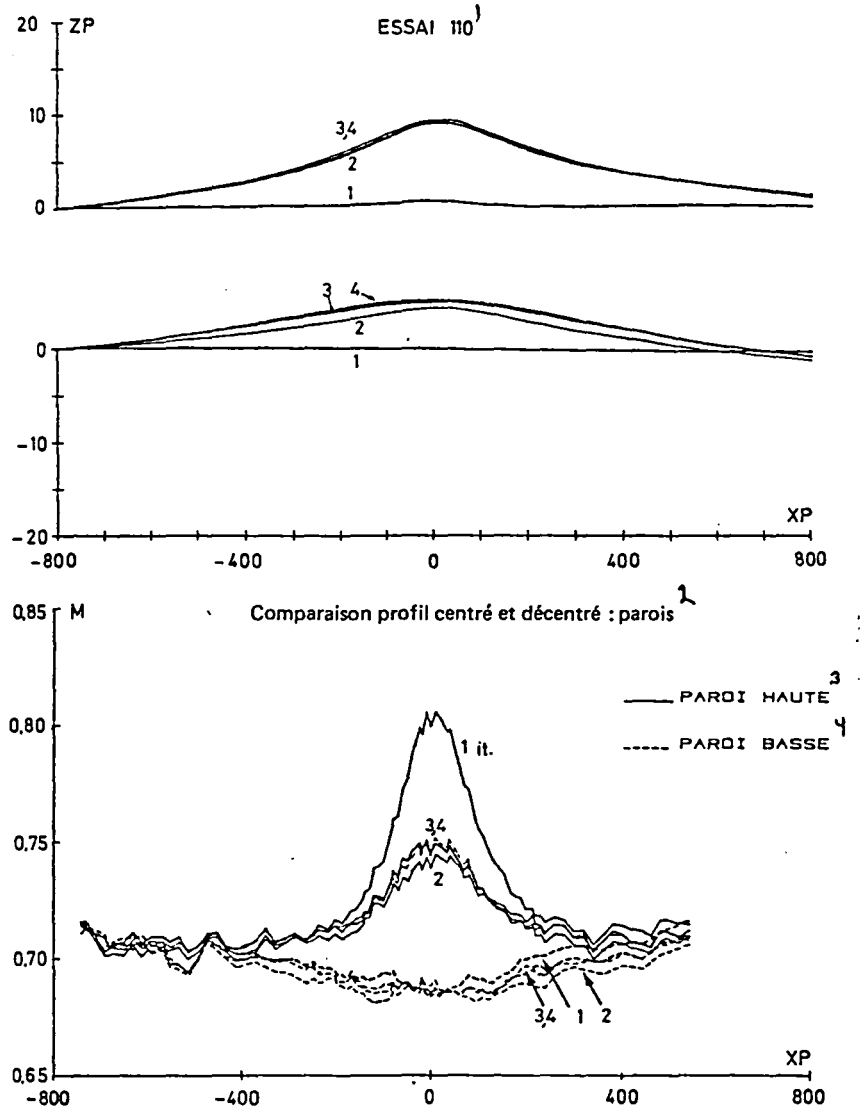

Figure 5. Development of distributions of local Mach numbers and wall shapes during iterative processes.

Key: 1-Test 110; 2-Centered and off-centered comparison: walls; 3-Upper wall; 4-Lower wall.

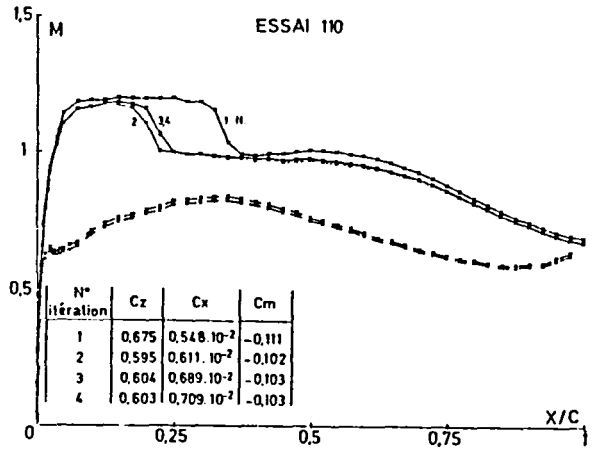

N° itération	Cz	Cx	Cm
1	0,675	0,548.10⁻²	-0,111
2	0,595	0,611.10⁻²	-0,102
3	0,604	0,689.10⁻²	-0,103
4	0,603	0,709.10⁻²	-0,103

Figure 6. Development of local Mach numbers on the profile during iterative processes and total coefficients.

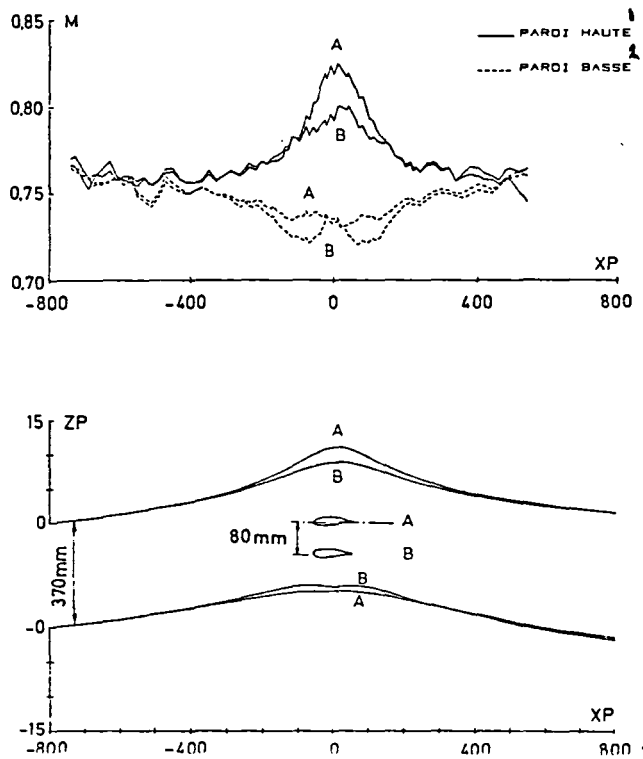

Figure 7. Comparison of Mach numbers and wall shapes for centered and off-centered profiles.

Key: 1-Upper wall; 2-Lower wall.

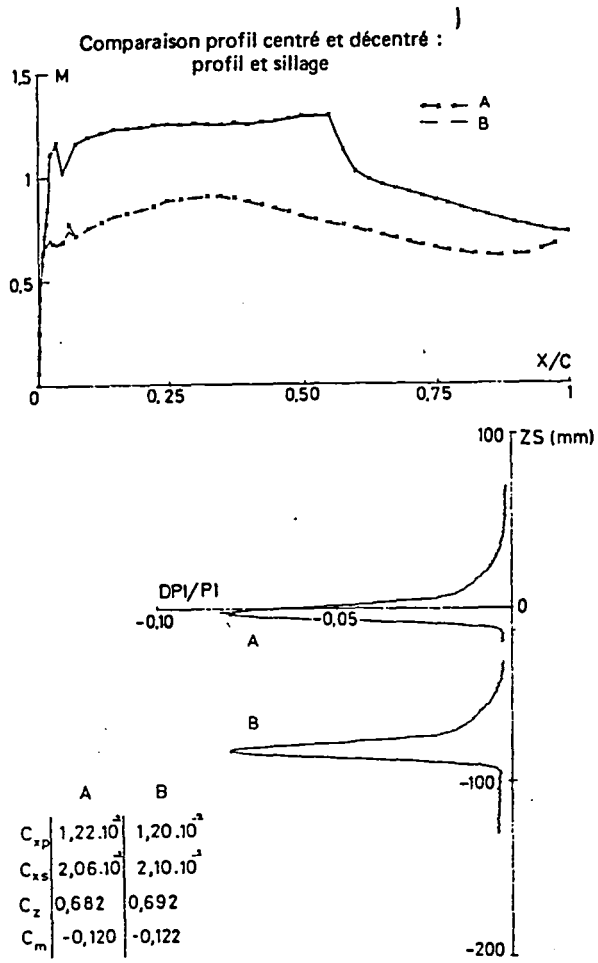

Figure 8. Local Mach numbers on the wash profile and total coefficients for CAST 7 profile and centered and off-centered position.

Key: 1-Centered and off-centered profile comparison: profile and wash.

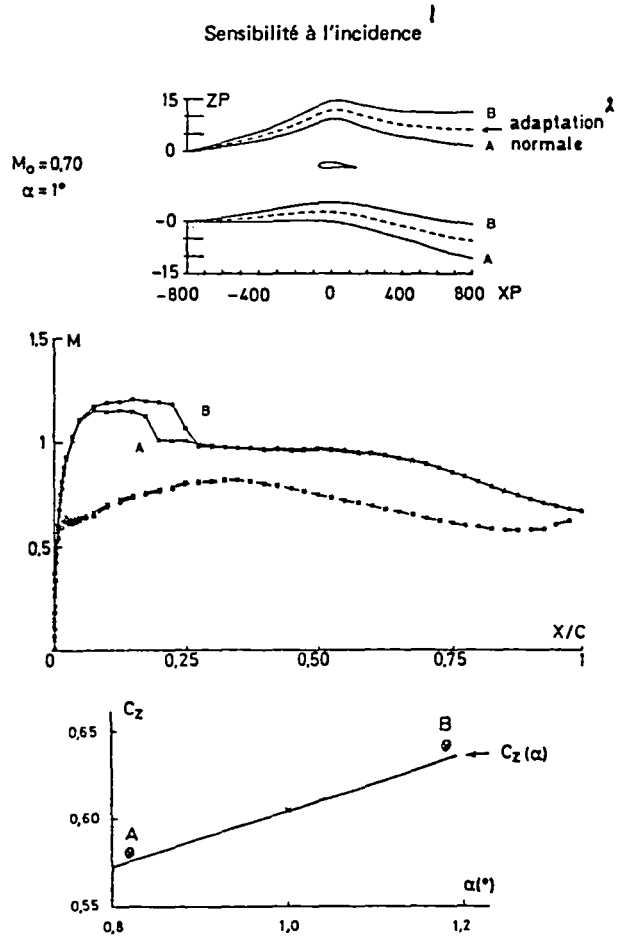

Figure 9. Effect of one rotation of the walls.

Key: 1-Sensitivity to incidence; 2-Normal adaptation.

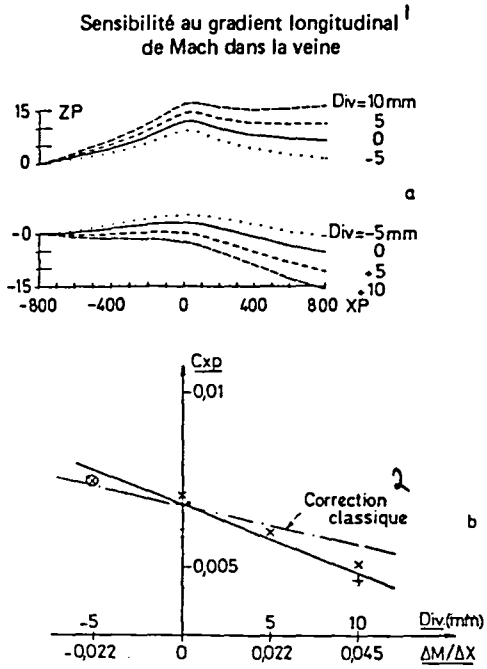

Figure 10. Effect of one divergence of the walls.

Key: 1-Sensitivity of the Mach longitudinal gradient in the section; 2-Standard correction.

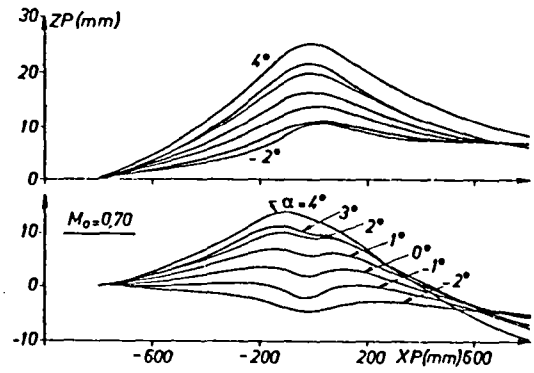

Figure 11. Wall shapes for various incidences of the model.

End of Document